# Subcarrier-Joint Pre- and Post-Equalization in Digital Subcarrier-Multiplexing Systems With Optical Filtering Impairments

Qiaoya Liu, *Graduate Student Member, IEEE*, Mengfan Fu, *Graduate Student Member, IEEE*, Xiaomin Liu, *Graduate Student Member, IEEE*, Xiaobo Zeng, Meng Cai, Hexun Jiang, Qizhi Qiu, Lilin Yi, Weisheng Hu, and Qunbi Zhuge, *Senior Member, IEEE, Senior Member, Optica*

***Abstract*—In this paper, the pre- and post-equalizers of all subcarriers are jointly optimized to compensate for optical filtering impairments caused by cascaded reconfigurable optical add-drop multiplexers (ROADMs) in digital subcarrier-multiplexing (SCM) systems. In the proposed scheme, equalizers of all subcarriers are jointly optimized based on a batch gradient descent algorithm and a novel loss function for a limited bit precision is designed to achieve the optimization. The performance is evaluated by extensive simulations in 4-subcarrier SCM systems with an aggregate symbol rate of 65 GBaud. Compared to current equalization schemes, the proposed scheme obtains generalized mutual information (GMI) gains of 0.1-0.3 bits/symbol after the transmission with 10 ROADMs in a linear channel with filtering penalties and amplified spontaneous emission (ASE) noise or a nonlinear channel where fiber nonlinearity and chromatic dispersion (CD) are introduced. The performance is also evaluated by experiments in 4-subcarrier SCM systems with an overall symbol rate of 32 GBaud. Transmission scenarios with different filtering impairments are emulated by a WaveShaper with different bandwidths. When the bandwidth of the WaveShaper is 26 GHz, the GMI gains of the proposed scheme over the current equalization schemes are 0.2–0.75 bits/symbol.**

***Index Terms*—Coherent optical transmissions, digital subcarrier-multiplexing systems, joint equalization, optical filtering impairments.**

## I. Introduction

With the rapid development of 5G communications, its applications such as cloud computing and data center interconnections have driven the development of flexible and high-capacity meshed optical networks [1], [2]. Reconfigurable optical add-drop multiplexers (ROADMs) which perform light path routing are key components in optical networks, and one ROADM typically consists of two wavelength selective switches (WSSs) [3]. However, optical filtering impairments induced by WSSs lead to inter-symbol interference (ISI) and thereby degrade the signal quality in long-haul transmission systems. The performance degradation becomes severer when the signal has to pass through several cascaded ROADMs because the transfer function will be significantly narrowed by a concatenation of filters [4], [5].

Several equalization algorithms used to compensate for optical filtering impairments have been proposed in single-carrier systems including the digital post-equalization [6], [7] and the joint optimization of the pre- and post-equalization [8], [9], [10]. When a post-equalizer in the receiver is applied alone [6], [7], low-power frequency components are emphasized during the ISI compensation and a large noise enhancement is introduced, leading to a signal-to-noise ratio (SNR) degradation. To solve the problem, a pre-equalizer is added in the transmitter [8], [9], [10] and jointly optimized with the post-equalizer. In [8], the pre-equalizer and the post-equalizer are jointly optimized to minimize the ISI. However, the ISI-free condition is not equivalent to the optimal received SNR because the received SNR is determined by both the ISI and the noise power. In [9], the channel transfer function is firstly estimated with a post-equalizer alone and then used as the frequency response of the pre-equalizer. After that, the post-equalizer is adaptively optimized again. In [10], pre- and post-equalizers are separately mapped to a one-dimensional convolutional layer and their weights are iteratively optimized to minimize the mean square error (MSE).

Recently, digital subcarrier-multiplexing (SCM) systems attract increasing attentions and have been implemented in the commercial application-specific integrated circuit (ASIC) for 800G digital signal processing (DSP) [11]. For SCM systems, the filtering effects induced by cascaded WSSs result in colored SNR distributions of subcarriers, which has been extensively studied [12], [13]. For systems with an identical modulation format for all subcarriers, the power loading can be used to improve the system performance [14], [15]. However, the gain is limited because the ISI in each subcarrier is also a main

Manuscript received 7 January 2024; revised 26 March 2024 and 13 May 2024; accepted 5 June 2024. Date of publication 14 June 2024; date of current version 16 October 2024. This work was supported in part by the Shanghai Pilot Program for Basic Research–Shanghai Jiao Tong University under Grant 21TQ1400213 and in part by the National Natural Science Foundation of China under Grant 62175145. *(Corresponding author: Qunbi Zhuge.)*

The authors are with the State Key Laboratory of Advanced Optical Communication Systems and Networks, Department of Electronic Engineering, Shanghai Jiao Tong University, Shanghai 200240, China (e-mail: lqy18039@sjtu.edu.cn; mengfan.fu@sjtu.edu.cn; xiaomin.liu@sjtu.edu.cn; xiaobo.zeng@sjtu.edu.cn; caimeng0922@sjtu.edu.cn; jianghexun@sjtu.edu.cn; qizhi.qiu@sjtu.edu.cn; lilinyi@sjtu.edu.cn; wsh@sjtu.edu.cn; qunbi.zhuge@sjtu.edu.cn).

Color versions of one or more figures in this article are available at https://doi.org/10.1109/JLT.2024.3414434.

Digital Object Identifier 10.1109/JLT.2024.3414434

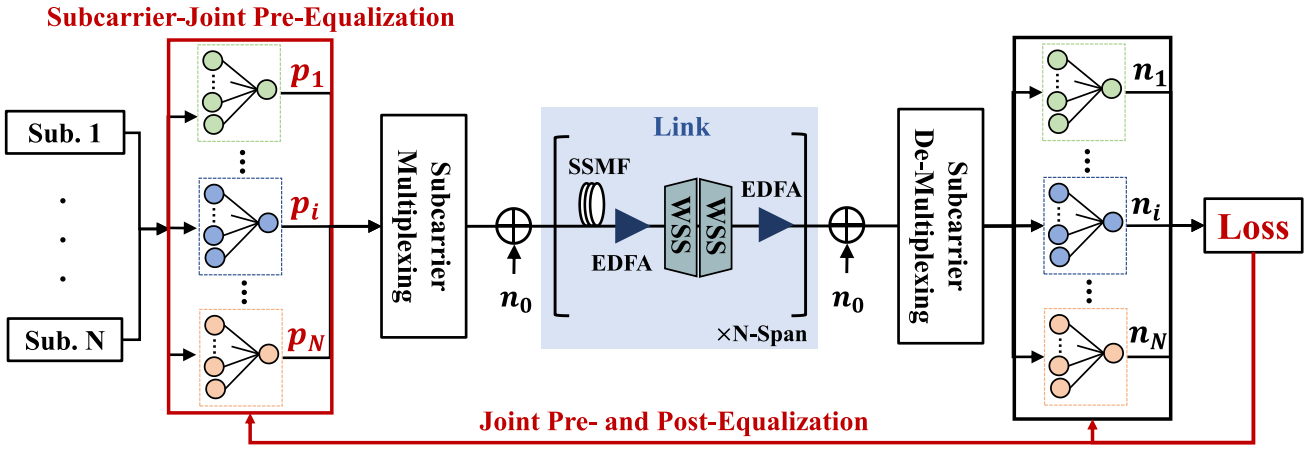


Fig. 1. The framework of the proposed subcarrier-joint pre- and post-equalization scheme.

influencing factor of the signal degradation. To compensate the ISI, the joint pre- and post-equalization in single-carrier systems [8], [9], [10] can be directly applied to SCM systems. However, the performance can be further improved. For systems with flexible modulation formats, the entropy loading can be used to improve the performance by allocating different modulation formats to subcarriers according to the SNR distribution [16], [17], [18]. In this paper, we focus on the former scenario, since commercial systems typically employ an identical modulation format over all subcarriers.

In digital SCM systems, optimizations of pre- and post-equalizers among all subcarriers are interactional and the joint pre- and post-equalization in digital SCM systems has not been studied. Besides, the MSE used in single-carrier systems cannot be directly used as the performance metric in digital SCM systems if the optimization target is maximizing the transmission rate.

In this paper, we propose a subcarrier-joint pre- and post-equalization scheme including a novel loss function to compensate for the filtering impairments in digital SCM systems. In the proposed equalization scheme, pre- and post-equalizers of all subcarriers are mapped to one-dimensional convolutional layers, and the equalizer weights are updated together to minimize the loss function based on a batch gradient descent algorithm. The performance of the proposed scheme is evaluated and analyzed by extensive simulations in 4-subcarrier systems with a total symbol rate of 65 GBaud. The generalized mutual information (GMI) gains of the proposed scheme over current equalization schemes are 0.1-0.3 bits/symbol after the transmission with 10 ROADMs in a linear or nonlinear channel. The performance of the proposed scheme is also evaluated by experiments in 4-subcarrier systems with a total symbol rate of 32 GBaud. Transmission scenarios with different filtering impairments are emulated by a WaveShaper (WS) with different bandwidths. Compared with current equalization schemes, the GMI gains of the proposed scheme are 0.2-0.75 bits/symbol when the bandwidth of the WS is 26 GHz.

The remainder of this paper is organized as follows. Section II introduces the principle of the proposed equalization scheme. In Section III, the performance is firstly analyzed by simulations in linear channels with filtering penalties and the additive white Gaussian noise (AWGN). Then the performance of the proposed scheme is validated by simulations in nonlinear channels where fiber nonlinearity and chromatic dispersion (CD) are further considered. Section IV presents experimental results. Finally, this paper is concluded in Section V.

**Algorithm 1:** The Optimization Procedure of the Subcarrier-Joint Pre- and Post-Equalization Scheme.

1. Generate a training dataset
2. Initialize the trainable weight matrices of pre- and post-equalizers of the $n$-th subcarrier: $\boldsymbol{w}_{1n}$ and $\boldsymbol{w}_{2n}$, $n = 1, \ldots, N$
3. For $i = 1, \ldots, N_{epoch}$
   For $j = 1, \ldots, N_{batch}$
   1) Do the forward propagation in Fig. 1
   2) Compute the loss function $L$
   3) Backpropagate and compute gradients of weights for each subcarrier
   $\nabla_{\boldsymbol{w}_{1n}} \boldsymbol{L}^{i,j}(w_{11}, \ldots, w_{1N}, w_{21}, \ldots, w_{2N})$ and
   $\nabla_{\boldsymbol{w}_{2n}} \boldsymbol{L}^{i,j}(w_{11}, \ldots, w_{1N}, w_{21}, \ldots, w_{2N})$
   End for
   1) Average the gradients of all batches as the gradients of $i$-th epoch $\nabla_{\boldsymbol{w}_{1n}} \boldsymbol{L}^{\boldsymbol{i}} = \frac{1}{N_{batch}} \sum_{j=1}^{N_{batch}} \nabla_{\boldsymbol{w}_{1n}} \boldsymbol{L}^{\boldsymbol{i,j}}$ and
   $\nabla_{\boldsymbol{w}_{2n}} \boldsymbol{L}^{\boldsymbol{i}} = \frac{1}{N_{batch}} \sum_{j=1}^{N_{batch}} \nabla_{\boldsymbol{w}_{2n}} \boldsymbol{L}^{\boldsymbol{i,j}}$
   2) Update weights of each subcarrier as
   $\boldsymbol{w}_{1n}^{i+1} = \boldsymbol{w}_{1n}^{i} - \mu \nabla_{\boldsymbol{w}_{1n}} \boldsymbol{L}^{\boldsymbol{i}}$ and
   $\boldsymbol{w}_{2n}^{i+1} = \boldsymbol{w}_{2n}^{i} - \mu \nabla_{\boldsymbol{w}_{2n}} \boldsymbol{L}^{\boldsymbol{i}}$
   End for

## II. Principle

In this section, the proposed subcarrier-joint pre- and post-equalization framework for digital SCM systems along with

its optimization procedure are firstly introduced. Then the loss function used in the optimization is derived.

### A. The Framework and the Optimization Procedure

Fig. 1 illustrates the proposed equalization framework in a digital SCM system with $N$ subcarriers. In the transmitter, generated symbols of each subcarrier are firstly upsampled to 2 samples per symbol (sps) and then jointly pre-equalized. After being multiplexed, fiber transmissions and being de-multiplexed, subcarriers are post-equalized in the receiver. In the proposed framework, each equalizer is independently mapped to a one-dimensional convolutional layer [10], and the joint equalization is achieved by maximizing the average GMI. In this procedure, the power of each subcarrier in the digital domain is not constrained and it is determined by the pre-equalizer weights. For each convolutional layer, the number of inputs equals the number of filter weights, and the output is the present-time filtered sample. In our simulations and experiments, sizes of all equalizer weights are the same and preset to 101.

Based on the proposed framework in Fig. 1, weights of all equalizers are updated by the Adam optimizer with the learning rate $\mu$ using a batch gradient descent algorithm. The optimization procedure in an N-subcarrier system is described in Algorithm 1. First, the training dataset used for optimizations is generated and the weights of all the equalizers are initialized. The weights of the pre-equalizer and the post-equalizer for the $n$-th subcarrier are denoted as $\boldsymbol{w_{1n}}$ and $\boldsymbol{w_{2n}}$. The initial values of $\boldsymbol{w_{1n}}$ and $\boldsymbol{w_{2n}}$ are set by matrices, of which the middle coefficient is 1 and others are small values close to 0. Next, the weight optimization process is performed $N_{epoch}$ epochs. $N_{epoch}$ is usually determined by observations and we make sure that it is enough for the convergence of weights. Each epoch includes $N_{batch}$ batches which is also pre-defined to satisfy the memory requirements of computations. For each batch, the forward propagation is performed as shown in Fig. 1 and the loss is calculated. Then the backpropagation is performed and gradients of the loss to the weights of all equalizers are computed based on the chain rule. When the optimization procedure is performed $N_{batch}$ batches, the gradients of all batches are averaged and the weights of all equalizers are updated.

### B. The Loss Function for Optimization

The optimization algorithm in Section II-A is applicable for any performance metrics. In this paper, we choose the system GMI under a fixed entropy as the performance metric which can reflect the effective transmission rate of systems. For digital SCM systems, the effective transmission rate is the sum of that of all subcarriers which are calculated as the products of GMI values and symbol rates. As symbols rates of subcarriers are the same in this paper, the system GMI is the average GMI of subcarriers. The average GMI can reflect the pre-soft-decision forward error correction (pre-SD FEC) performance of digital SCM systems [19]. However, if the average GMI is directly used for the equalizer optimization, the calculation of gradients will overflow. To address this problem, a novel loss function used in Algorithm 1 is designed and introduced in this part.

The average GMI of subcarriers $\overline{GMI}$ is calculated as (1) [20], where the first term is the average entropy of subcarriers and the second term indicates the impact of channel noises. $N$ is the subcarrier number and $l$ is the symbol length. $x_{n,k}$ is the $k$-th transmitted symbol of the $n$-th subcarrier and $P_X(x_{n,k})$ is the probability of $x_{n,k}$. $b_{n,k,i}$ is the $i$-th bit of $x_{n,k}$. $m = log_2(M)$ and $M$ is the order of the adopted quadrature amplitude modulation (QAM) format. $\Lambda_{n,k,i}$ is the soft bit-wise de-mapper output and it is computed as [20]:

$$\overline{GMI} = \frac{1}{l \times N} \sum_{n=1}^{N} \sum_{k=1}^{l} \left[-log_2\left(P_X\left(x_{n,k}\right)\right)\right] - \frac{1}{l \times N} \sum_{n=1}^{N} \sum_{k=1}^{l} \sum_{i=1}^{m} log_2\left(1 + e^{(-1)^{b_{n,k,i}} \Lambda_{n,k,i}}\right) \tag{1}$$

$$\Lambda_{n,k,i} = log \frac{\sum_{x_n \in \chi_1^i} e^{-\frac{\left|y_{n,k} - x_n\right|^2}{2\sigma_n^2}} P_X\left(x_n\right)}{\sum_{x_n \in \chi_0^i} e^{-\frac{\left|y_{n,k} - x_n\right|^2}{2\sigma_n^2}} P_X\left(x_n\right)} \tag{2}$$

where $y_{n,k}$ is the $k$-th received symbol and $\sigma_n^2$ is the noise variance of the auxiliary channel for the $n$-th subcarrier. $\chi_1^i$ and $\chi_0^i$ denote the set of constellation points whose $i$-th bit is 1 and 0, respectively.

Based on (1), the second term can be used as the loss function to maximize the average GMI of subcarriers. However, the overflow may happen in this case because the gradient of $\Lambda_{n,k,i}$ to the denominator of the anti-logarithm in (2) can be negative infinity, especially for bit precisions lower than 64-bit. The bit precision used in this paper is 32-bit. The denominator is determined by both modulation formats and SNR, and the overflow can easily occur in practical configurations for both probabilistically shaped (PS) QAM signals and standard uniform QAM signals. Taking the PS 64-QAM format with an entropy of 5 bits/symbol for example, the overflow occurs when the SNR is larger than 10 dB (GMI is 3.3 bits/symbol). For the uniform 64-QAM format, the overflow occurs when the SNR is larger than 13 dB (GMI is 3.7 bits/symbol). To avoid the overflow, the GMI can be approximately calculated in the logarithmic scale [21]. However, the approximation will lead to a performance degradation. Therefore, we propose a new approach to address this problem as described in the following.

First, $\sigma_n^2$ in (2) is multiplied by a constant $\alpha$ which is larger than 1, as shown in (3). In this paper, $\alpha$ of all subcarriers is set to 30 which is determined to avoid the overflow for all subcarriers. After introducing $\alpha$, the quasi-GMI based on (3) deviates from the real GMI based on (2). As shown in Fig. 2, the right ordinate is the quasi-GMI based on (3) and the left ordinate is the deviation in GMI which is calculated as the ratio of the real GMI based on (2) to the quasi-GMI based on (3). For a fixed $\alpha$, the deviations in GMI of signals with different SNRs are different. In the SCM system with cascaded ROADMs, SNRs of subcarriers are different and thus the deviations in GMI of subcarriers are different. In this case, the average of the quasi-GMI based on (3) is not proportional to the real average GMI and Algorithm 1 will converge to a local optimum. Therefore, we further propose

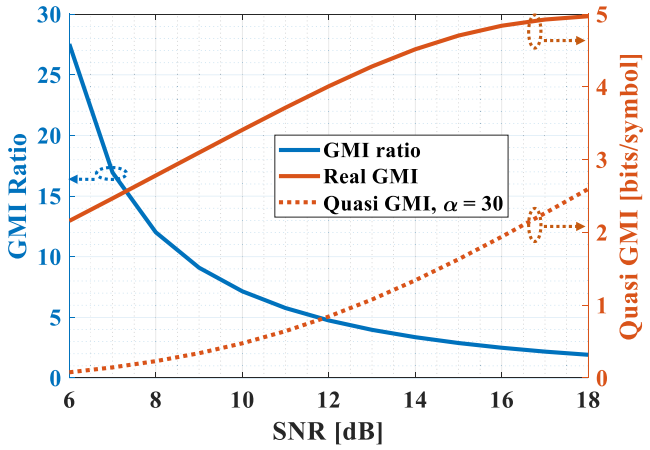


Fig. 2. Deviations in GMI with SNR, taking $\alpha$ of 30 for example.

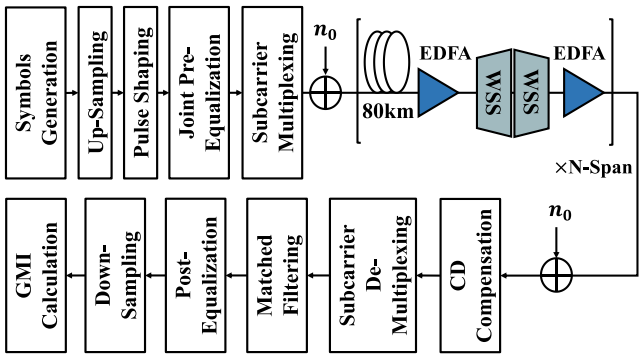


Fig. 3. Simulation setup.

to multiply the channel noise term of the $n$-th subcarrier by a factor $\beta_n$ to make sure that the average of the quasi-GMI is proportional to the real average GMI. Finally, the loss function is derived as (4) where $\beta_n$ is not restricted to fixed values, as long as the combinations of $\beta_n$ enable the loss function to be proportional to the second term of (1).

$$\Lambda'_{n,k,i} = log\frac{\sum_{x_n\in\chi_1^i} e^{-\frac{\left|y_{n,k}-x_n\right|^2}{2\sigma_n^2\alpha}} P_X(x_n)}{\sum_{x_n\in\chi_0^i} e^{-\frac{\left|y_{n,k}-x_n\right|^2}{2\sigma_n^2\alpha}} P_X(x_n)} \tag{3}$$

$$\begin{aligned} Loss &= \sum_{n=1}^{N}\left(\left(\sum_{k=1}^{l}\sum_{i=1}^{m} log_2\left(1+e^{(-1)^{b_{n,k,i}}\Lambda'_{n,k,i}}\right)\right)\times\beta_n\right) \\ &\propto \sum_{n=1}^{N}\left(\sum_{k=1}^{l}\sum_{i=1}^{m} log_2\left(1+e^{(-1)^{b_{n,k,i}}\Lambda_{n,k,i}}\right)\right) \end{aligned} \tag{4}$$

In the proposed scheme, based on the SNR distribution of the post-equalization scheme, $\alpha$ is firstly predetermined to ensure that the gradient calculations of all subcarriers do not overflow. Then an initial $\beta_n$ is determined for the $n$-th subcarrier, based on the relationship between $\alpha$ and $\beta$ in Fig. 2. Next, the optimization based on Algorithm 1 is performed and $\beta_n$ is updated based on the optimized SNR distribution in the previous optimization loop. Finally, after several iterations, the optimized $\beta_n$ and equalizer weights are obtained. In our simulations and experiments, we observe that six iterations are usually sufficient.

## III. Simulation Results

### A. The Simulation Setup

The performance of the proposed scheme is evaluated by extensive simulations in a 4-subcarrier system under a fixed system transmission rate. The simulation setup is depicted in Fig. 3. Transmitted symbols of each subcarrier are firstly generated based on the PS 64-QAM format with an entropy of 5 bits/symbol. After being up-sampled and shaped by a 64-tap root raised-cosine (RRC) filter with a roll-off factor of 0.1, all subcarriers are jointly pre-equalized and then multiplexed to an SCM signal with an aggregate symbol rate of 65 GBaud. The symbol rate and the spacing of each subcarrier are 16.25 GBaud and 17.875 GHz, respectively. The back-to-back (BTB) SNR of 18 dB is emulated by loading equal amounts of AWGN in the transmitter and receiver. The transmission link consists of standard single-mode fiber (SSMF), erbium-doped fiber amplifiers (EDFAs) and ROADMs. The fiber length of each span is 80 km. An EDFA with a noise figure of 5 dB and a gain of 16 dB is inserted after each span to compensate for the fiber loss. Then a ROADM is inserted followed by an EDFA which is used to ensure a constant signal launch power of each span. A ROADM consists of two WSSs [3] and the transfer function of each WSS is emulated as (5)–(6) [22].

$$S(f) = \frac{1}{2}\delta\sqrt{2\pi}\left\{erf\left(\frac{\frac{B_0}{2}-f}{\sqrt{2}\sigma}\right) - erf\left(\frac{-\frac{B_0}{2}-f}{\sqrt{2}\sigma}\right)\right\} \tag{5}$$

$$\delta = \frac{B_{OTF}}{2\sqrt{2ln2}} \tag{6}$$

where $B_0$ is the bandwidth of the WSS and it is set to 75 GHz in the simulations. $B_{OTF}$ is the 3-dB bandwidth of the Gaussian optical transfer function and it is set to 12 GHz.

In the simulations, two link channels are considered: 1) the linear channel where only the optical filtering, fiber loss and amplified spontaneous emission (ASE) noises are considered; 2) the nonlinear channel where fiber nonlinearity and CD are further introduced. The equalization performance of the proposed scheme is comprehensively analyzed in the linear channel and then validated in the nonlinear channel. In the receiver, after subcarrier de-multiplexing, matched filtering and the post-equalization are implemented. Finally, the GMI of each subcarrier is calculated. It is noted that the CD compensation is only conducted in the second link scenario.

To analyze the performance of the proposed scheme, the following four schemes are adopted for comparison: 1) the traditional equalization scheme with the post-equalization alone for each subcarrier, denoted by "Post"; 2) the joint pre-

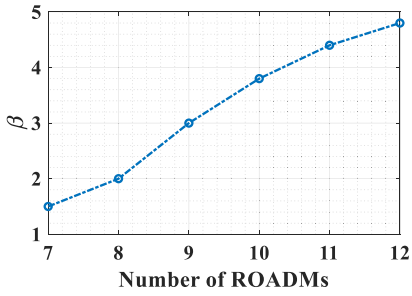


Fig. 4. Optimized $\beta$ of the edge subcarriers with the proposed scheme in the linear channel.

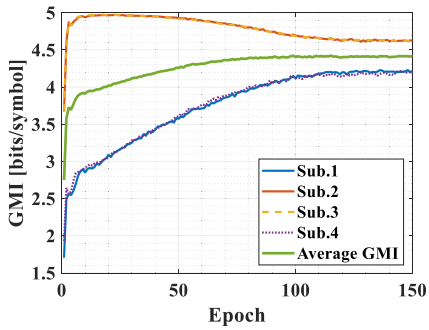


Fig. 5. The GMI convergence curves of the proposed scheme for the transmission with 7 ROADMs.

and post-equalization for each subcarrier separately [10], denoted by "Pre+Post-EachSub."; 3) the scheme where the post-equalization is firstly performed followed by the power loading with one scale factor for each subcarrier, denoted by "Post+PL"; 4) the scheme where the separate pre- and post-equalization for each subcarrier is firstly performed followed by the power loading, denoted by "(Pre+Post-EachSub.)+PL".

### B. Results of Transmissions in the Linear Channel

In this part, the GMI gains of the proposed scheme over the other four schemes are evaluated in the channel with filtering impairments and ASE noise, and the launch power is set to 0 dBm.

In the simulations, as mentioned earlier, $\alpha$ is set to 30 and $\beta$ in (4) are optimized by a binary search method. As the frequency offset is not considered, $\beta_n$ of symmetrical subcarriers are set to the same values. Based on the analysis of (4), $\beta_n$ are not restricted to fixed values, as long as the loss function is proportional to the second term of (1). Therefore, $\beta_{2,3}$ of the center subcarriers is fixed to 1 and only the optimized $\beta_{1,4}$ of the edge subcarriers is shown in Fig. 4. Compared with the center subcarriers, the SNR of the edge subcarriers is lower and thus $\beta_{1,4}$ is larger based on Fig. 2. For severer filtering impairments, the SNR difference between the center and edge subcarriers is larger and thus the difference of $\beta$ is larger based on Fig. 2. As shown in Fig. 4, $\beta_{1,4}$ of the edge subcarriers increases with the number of ROADMs.

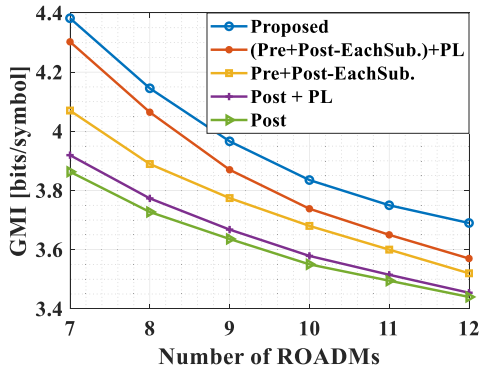


Fig. 6. The average GMI of the five schemes in the linear channel.

Fig. 5 shows the GMI convergence curves of the proposed scheme, taking the transmission with 7 ROADMs for example. The average GMI converges after 120 epochs and subcarriers with symmetrical center frequencies converge to very similar performance. The initial increase of SNR of all subcarriers is attributed to the ISI compensation. Later, since the SNR of the center subcarriers is larger, their powers are transferred to the edge subcarriers. During this process, the ISI compensation is further optimized.

The average GMI of the five schemes are compared in Fig. 6. Taking the transmission with 10 ROADMs for example, the GMI gains of the proposed scheme over Post, Post+PL, Pre+Post-EachSub., and (Pre+Post-EachSub.)+PL are 0.3, 0.26, 0.16, and 0.1 bits/symbol, respectively. Compared with Post, Post+PL transfers the power from the center subcarriers to the edge subcarriers to improve the average GMI. However, the gain is limited because there is no futher compensation for the ISI which is the main factor of the signal degradation. Compared with Post, Pre+Post-EachSub. reduces the noise enhancement in the receiver and obtains partial gains. However, the equalizer weights of each subcarrier are optimized separately and the optimization among subcarriers is not considered in Pre+Post-EachSub.. In this case, the average GMI of SCM systems is restricted by the GMI of the edge subcarriers with severe filtering impairments, and thus the performance of Pre+Post-EachSub. is limited. For (Pre+Post-EachSub.)+PL, the interplay of subcarrier powers and the pre- and post-equalization is not considered, and there is still a performance gap. Finally, in the proposed scheme, the performance gap is filled by the joint optimization of subcarrier powers and the pre- and post-equalization.

The power optimization results of Post+PL, (Pre+Post-EachSub.)+PL and the proposed scheme are shown in Fig. 7(a), where the ordinate is the relative power of the edge subcarriers and the sum of all subcarriers is 1. Fig. 7(a) shows that compared with the center subcarriers, more powers are allocated to the edge subcarriers for all the transmission scenarios. This is because the GMI of the center subcarrier is larger than that of the edge subcarriers when the powers of the subcarriers are identical, and some powers can be transferred from the center subcarriers to the edge subcarriers to obtain a larger average GMI. For a larger number of ROADMs, the SNR of the edge subcarriers is

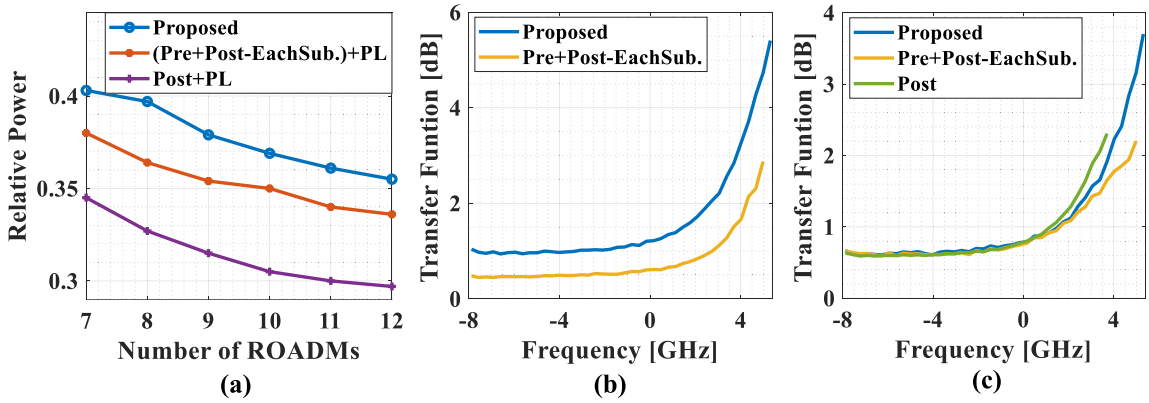


Fig. 7. (a) The optimized power of the edge subcarriers for Post+PL, (Pre+Post-EachSub.)+PL and the proposed scheme. The optimized transfer functions of the edge subcarrier after the transmission with 10 ROADMs: (b) the pre-equalizers and (c) the post-equalizers.

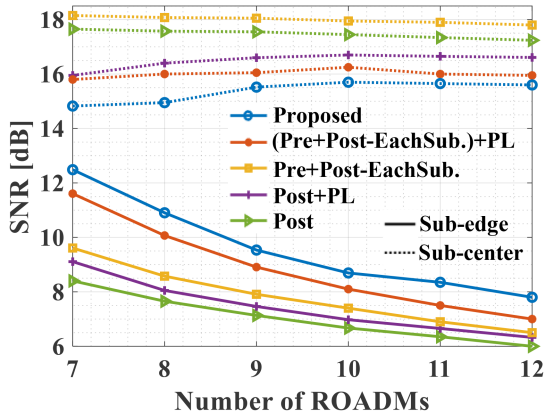


Fig. 8. The SNR distributions of the five schemes.

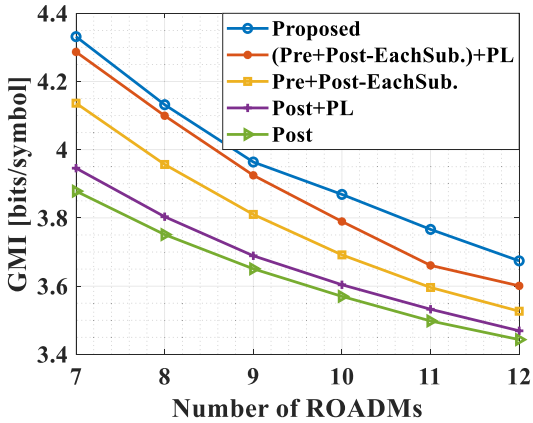


Fig. 9. The average GMI of the five schemes in the nonlinear channel.

degraded more severely and less GMI gain can be obtained by the power transfer. As a result, in Fig. 7(a), the power of the edge subcarriers decreases with the number of ROADMs. Compared with Post+PL and (Pre+Post-EachSub.)+PL, the SNR of the edge subcarriers in the proposed scheme is further improved by the joint optimization of subcarrier powers and the pre- and post-equalization. Correspondingly, more power is transferred based on the proposed scheme in Fig. 7(a).

The optimized transfer functions of pre- and post-equalizers of the five schemes are shown in Fig. 7(b) and Fig. 7(c), respectively, taking the transmission with 10 ROADMs for example. Note that the post-equalizers of Post+PL and Post are the same, and pre- and post-equalizers of Pre+Post-EachSub. and (Pre+Post-EachSub.)+PL are the same. Besides, since the frequency offset is not considered and the center subcarriers are not affected by the filtering, only transfer functions of the edge subcarriers are provided. In Fig. 7(b), the transfer function values of the proposed scheme are larger compared with Pre+Post-EachSub., because it contains the power loading. Meanwhile, based on the joint optimization of subcarrier powers and equalizer weights, the post-equalizers of the proposed scheme have a higher equalization degree compared with Pre+Post-EachSub., as shown in Fig. 7(c). This is because the additive noise of the edge subcarriers is equivalently smaller and more equalization can be applied after the power transfer to the edge subcarriers. Note that the equalization degree is defined by the relative magnitudes of frequency points in this paper.

Fig. 8 compares the SNR distributions of the five schemes where the SNRs of subcarriers with symmetrical center frequencies are averaged. Compared with Post, Pre+Post-EachSub. obtains a gain of about 1 dB for the SNR of the edge subcarriers after each subcarrier is jointly pre- and post-equalized. For the proposed scheme, the SNR gain of the edge subcarriers is larger by jointly optimizing the power, the pre- and post-equalizer weights of all subcarriers, and the SNR distributions are consistent with the power optimization results in Fig. 7(a).

### C. *Results of Transmissions in the Nonlinear Channel*

In this part, the performance of the proposed scheme is validated in a single channel where fiber nonlinearity and CD are introduced, and all equalizer weights are re-optimized for all the transmission scenarios. For the nonlinear channel, the fiber is simulated based on the split-step Fourier method (SSFM) and the step size is 20 m. The optimal launch power is $-1$ dBm.

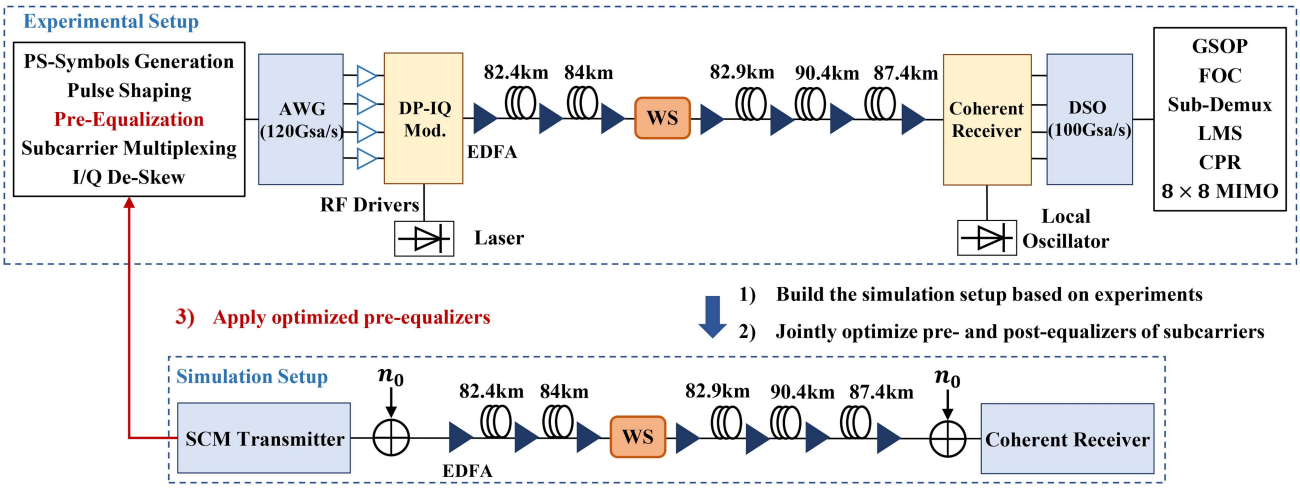


Fig. 10. The experimental setup.

As the performance of the proposed scheme has been analyzed comprehensively in the linear channel and the analysis in the nonlinear channel is similar, only the average GMI results of the five schemes are presented in this part. As shown in Fig. 9, the results of linear and nonlinear transmissions are similar. This is because the fiber nonlinear noise is similar to AWGN [23], and the change of signal spectrum due to the pre-equalization is relatively small, which does not affect the amount of the fiber nonlinear noise [14]. Taking the transmission with 10 ROADMs for example, the GMI gains of the proposed scheme over Post, Post+PL, Pre+Post-EachSub., and (Pre+Post-EachSub.)+PL are 0.3, 0.26, 0.16, and 0.1 bits/symbol, respectively.

## IV. Experimental Results

In this section, the performance of the proposed scheme is experimentally demonstrated in 4-subcarrier SCM systems with an aggregate symbol rate of 32 GBaud. The symbol rate and the spacing of each subcarrier are 8 GBaud and 9 GHz, respectively. The BTB-SNR is 18 dB and scenarios with different filtering impairments are emulated by a WS with different bandwidths [17], [18]. To aid the optimization, a simulation setup is built by setting the same configurations of filtering impairments and noises as the experimental setup, including the transceiver noise, fiber parameters and filter shapes of the WS. The transceiver noise such as the quantization noise is emulated by AWGN and equally loaded at the transmitter and the receiver. Note that the transceiver bandwidth is not considered in the offline simulation because it is sufficiently large in our transmissions. Then all the filter weights are optimized offline based on this simulation setup and finally used in the experiment. Finally, the average GMI of each experimental transmission scenario is calculated.

### A. The Experimental Setup

The experimental setup and DSP procedures are depicted in Fig. 10. In the transmitter, PS 64-QAM symbols with an entropy of 5 bits/symol for each subcarrier are firstly generated in MATLAB. After being up-sampled and shaped by a 64-tap RRC filter with a roll-off factor of 0.1, the subcarriers are pre-equalized and then multiplexed to an SCM signal. Then the In-phase/Quadrature (I/Q) de-skew is performed to compensate the delay between I and Q components in the transmitter. The generated digital SCM signals are sent to an arbitrary waveform generator (AWG) with a sampling rate of 120 GSa/s and then modulated by a dual-polarization I/Q modulator (DP-I/Q Mod.). A tunable external-cavity laser (ECL) with a center frequency of 193.4 THz is adopted and the nominal linewidth is 100 kHz. Then the output optical signal is amplified by an EDFA. The optimal launch power of signals is 3 dBm. In the transmission link, the signal passes through five spans with a total length of 427 km and a WS with variable bandwidths. An EDFA is inserted after each span and the WS to compensate for the fiber loss and the insertion loss. In the receiver, the received optical signal is converted into four electrical signals by an integrated coherent receiver and another ECL with a nominal linewidth of 100 kHz is used as a local oscillator. The electrical signals are sampled by a digital storage oscilloscope (DSO) with a sampling rate of 100 GSa/s.

The received digital SCM signals are processed offline. Firstly, the Gram-Schmidt orthogonalization procedure (GSOP) is performed, followed by the frequency offset compensation (FOC). After the subcarriers are de-multiplexed (Sub-Demux), the least mean square (LMS) and carrier phase recovery (CPR) are carried out. Then an $8 \times 8$ real-valued post-equalizer ($8 \times 8$ MIMO) is employed to compensate for the residual IQ errors from the transmitter [24].

### B. Experimental Results

As the analysis of the experimental results is similar to that of Section III, only the average GMI of the five schemes are presented in this part. Applying the optimized pre-equalizers obtained based on the simulation setup to experiments, the average GMI of the five schemes are shown in Fig. 11. When the bandwidth of the WS is 26 GHz, the GMI gains of the proposed scheme over Post, Pre+Post-EachSub., Post+PL

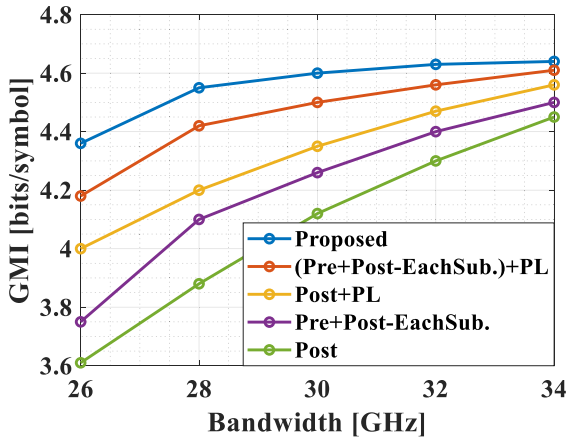


Fig. 11. The average GMI of the five schemes in experiments.

and (Pre+Post-EachSub.)+PL are 0.75, 0.6, 0.35 and 0.2 bits/symbol, respectively. Different from the simulation results in Section III, the performance of Post+PL is better than Pre+Post-EachSub.. This is because the SNR of the edge subcarriers is larger (9∼13 dB) than that in the simulations (<8 dB). In this case, a larger average GMI gain is obtained by the power transfer based on Post+PL.

## V. Conclusion

In this paper, we propose a subcarrier-joint pre- and post-equalization scheme including a novel loss function used for the optimization of equalizer weights. The proposed loss function is particularly necessary for a limited bit precision. Considering the interplay of subcarrier powers and the relative values of equalizer weights, the proposed scheme jointly optimizes pre- and post-equalizers of all subcarriers and obtains gains over current equalization schemes. Extensive simulations and experiments are performed to comprehensively evaluate the performance of the proposed scheme. In the simulations with linear or nonlinear channels, after the transmission with 10 ROADMs, the GMI gains of the proposed scheme over Post, Post+PL, Pre+Post-EachSub., and (Pre+Post-EachSub.)+PL schemes are 0.3, 0.26, 0.16, and 0.1 bits/symbol, respectively. In the experiments, when the bandwidth of the WS is 26 GHz, the GMI gains of the proposed scheme over Post, Pre+Post-EachSub., Post+PL and (Pre+Post-EachSub.)+PL schemes are 0.75, 0.6, 0.35 and 0.2 bits/symbol, respectively.

## References

[1] Z. Feng, H. Chen, F. Shi, Y. Jia, Q. Wu, and H. Shi, "ROADM traversal improvement enabled by optical domain equalization," in *Proc. IEEE Optoelectron. Glob. Conf.*, 2021.

[2] M. Benisha, R. T. Prabu, and V. T. Bai, "Requirements and challenges of 5G cellular systems," in *Proc. IEEE 2nd Int. Conf. Adv. Elect., Electron., Inf., Commun. Bio-Inform.*, 2016, pp. 251–254.

[3] B. Clouet et al., "Networking aspects for next-generation elastic optical interfaces," *J. Opt. Commun. Netw.*, vol. 8, no. 7, pp. A116–A125, Jul. 2016.

[4] J.M. Fabrega et al., "On the filter narrowing issues in elastic optical networks," *J. Opt. Commun. Netw.*, vol. 8, no. 7, pp. A23–A33, Jul. 2016.

[5] T. Zami, I. F. de Jauregui Ruiz, A. Ghazisaeidi, and B. Lavigne, "Growing impact of optical filtering in future WDM networks," in *Proc. IEEE Opt. Fiber Commun. Conf.*, 2019, pp. 1–3.

[6] L. Li, A. I. Abd El-Rahman, and J. C. Cartledge, "Effect of bandwidth narrowing due to cascaded wavelength selective switches on the generalized mutual information of probabilistically shaped 64-QAM systems," in *Proc. IEEE Eur. Conf. Opt. Commun.*, 2018, pp. 1–3.

[7] P. A. Loureiro et al., "WSS filtering penalties with bandwidth-variable transceivers: On the debate between single- and multi-carrier," in *Proc. Eur. Conf. Opt. Commun.*, 2022, Paper Th2C.3.

[8] Y. Mori, H. Hasegawa, and K. Sato, "Joint pre-, inline-, and post-compensation of spectrum narrowing caused by traversing multiple optical nodes," in *Proc. IEEE Eur. Conf. Opt. Commun.*, 2017, pp. 1–3.

[9] J. Zhang, J. Yu, N. Chi, and H. Chien, "Time-domain digital pre-equalization for band-limited signals based on receiver-side adaptive equalizers," *Opt. Exp.*, vol. 22, no. 17, pp. 20515–20529, 2014.

[10] Z. Zhai et al., "An interpretable mapping from a communication system to a neural network for optimal transceiver-joint equalization," *J. Lightw. Technol.*, vol. 39, no. 17, pp. 5449–5458, 2021.

[11] H. Sun et al., "800G DSP ASIC design using probabilistic shaping and digital sub-carrier multiplexing," *J. Lightw. Technol.*, vol. 38, no. 17, pp. 4744–4756, 2020.

[12] P.A. Loureiro et al., "On the mitigation of WSS filtering penalties: Single- vs multi-carrier modulation," *J. Lightw. Technol.*, vol. 41, no. 11, pp. 3628–3634, 2023.

[13] P. A. Loureiro et al., "WSS filtering penalties with bandwidth-variable transceivers: On the debate between single- and multi-carrier," in *Proc. Eur. Conf. Opt. Commun.*, 2022, Paper Th2C.3.

[14] A. M. R. Brusin, F. P. Guiomar, A. Lorences-Riesgo, P. P. Monteiro, and A. Carena, "Enhanced resilience towards ROADM-induced optical filtering using subcarrier multiplexing and optimized bit and power loading," *Opt. Exp.*, vol. 27, no. 21, pp. 30710–30725, 2019.

[15] F. P. Guiomar, A. Lorences-Riesgo, A. M. Rosa Brusin, D. F. Morillo, A. Carena, and P. P. Monteiro, "Reducing ROADM filtering penalties using subcarrier multiplexing with offline bit and power loading," in *Proc. IEEE Eur. Conf. Opt. Commun.*, 2018, pp. 1–3.

[16] D. Che and W. Shieh, "Approaching the capacity of colored-SNR optical channels by multicarrier entropy loading," *J. Lightw. Technol.*, vol. 36, no. 1, pp. 68–78, 2018.

[17] D. Che and W. Shieh, "Squeezing out the last few bits from band-limited channels with entropy loading," *J. Lightw. Technol.*, vol. 27, no. 7, pp. 9321–9329, 2019.

[18] Q. Liu et al., "Subcarrier-pairing entropy loading for digital subcarrier-multiplexing systems with colored-SNR distributions," *Opt. Exp.*, vol. 29, no. 18, pp. 28852–28863, 2021.

[19] J. Cho, L. Schmalen, and P. J. Winzer, "Normalized generalized mutual information as a forward error correction threshold for probabilistically shaped QAM," in *Proc. IEEE Eur. Conf. Opt. Commun.*, 2017, pp. 1–3.

[20] T. Fehenberger, A. Alvarado, G. Böcherer, and N. Hanik, "On probabilistic shaping of quadrature amplitude modulation for the nonlinear fiber channel," *J. Lightw. Technol.*, vol. 34, no. 21, pp. 5063–5073, 2016.

[21] P. Robertson, E. Villebrun, and P. Hoeher, "A comparison of optimal and sub-optimal MAP decoding algorithms operating in the log domain," in *Proc. IEEE Int. Conf. Commun.*, 1995, pp. 1009–1013.

[22] C. Pulikkaseril, L. A. Stewart, M. A. F. Roelens, G. W. Baxter, S. Poole, and S. Frisken, "Spectral modeling of channel band shapes in wavelength selective switches," *Opt. Exp.*, vol. 19, no. 9, pp. 8458–8470, 2011.

[23] P. Poggiolini, G. Bosco, A. Carena, V. Curri, Y. Jiang, and F. Forghieri, "The GN-model of fiber non-linear propagation and its applications," *J. Lightw. Technol.*, vol. 32, no. 4, pp. 694–721, 2014.

[24] Z. Zhai et al., "Transmitter IQ mismatch compensation and monitoring for digital subcarrier-multiplexing system," in *Proc. Asia Commun. Photon. Conf.*, 2020, Paper S4C. 3.